Polymer 49 (2008) 4559–4568

Contents lists available at ScienceDirect

Polymer

journal homepage: www.elsevier.com/locate/polymer

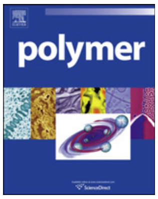

Synthesis and properties of various PPV derivatives with phenyl substituents

Youngeup Jin [a], Suhee Song [a], Sung Heum Park [b], Jin-A Park [a], Jinwoo Kim [a], Han Young Woo [c], Kwanghee Lee [b], Hongsuk Suh [a,*]

[a] *Department of Chemistry, Chemistry Institute for Functional Materials, Pusan National University, Pusan 609-735, Republic of Korea*
[b] *Department of Materials Science and Engineering Gwangju Institute of Science and Technology Gwangju 500-712, Republic of Korea*
[c] *Department of Nanomaterials Engineering, Pusan National University, Miryang 627-706, Republic of Korea*

ARTICLE INFO

Article history:
Received 21 June 2008
Received in revised form 15 August 2008
Accepted 18 August 2008
Available online 27 August 2008

Keywords:
PPV derivatives
Phenyl substituents
Polymer light-emitting diodes

ABSTRACT

New electroluminescent polymers with various phenyl groups, poly[2-dimethyl(octyl)silyl-5-(4-(dimethyl(octyl)silyl)phenyl)-1,4-phenylenevinylene] (**P1**), poly[2,5-bis(4-(dimethyl(octyl)silyl)phenyl)-1,4-phenylenevinylene] (**P2**), poly[2,5-bis(9,9-dihexylfluorenyl)-1,4-phenylenevinylene] (**P3**), and poly [2,5-bis(4-(4-(2-etylhexyloxy)phenyl)phenyl)-1,4-phenylenevinylene] (**P4**), have been synthesized by the Gilch polymerization. The maximum absorption peaks of **P1**–**P4** appeared at 388–423 nm in THF solution, and are red-shifted to 404–425 nm in solid thin film. The photoluminescence (PL) emission spectra of **P1**–**P4** show a maximum peak at 482–503 nm in THF solution and at 521–549 nm as the solid film state. The emission spectra in the solid film state are more red-shifted over 40 nm, and the full width at half maximum (fwhm) was 30 nm greater than the solution conditions. The polymer light-emitting diodes (PLEDs) with the configuration of ITO/PEDOT/polymer/Al emitted light with maximum peaks at around 517–546 nm. The various phenyl substituents, with intermolecular interactions in the solid film state, can introduce the color tuning and device performance enhancement of the conjugated polymer as an emissive layer in PLED.

1. Introduction

Organic light-emitting diodes (OLEDs) have been researched extensively in full color flat panel displays, with several advantages over conventional devices such as a low driving voltage, wide viewing angle, thin film structure, and a simpler manufacturing process [1–3]. After the discovery of electroluminescence (EL) from conjugated polymers, numerous reports about polymer light-emitting diodes (PLEDs) have been published since π-conjugated polymeric materials are slated to possess interesting and useful electronic and optical properties [4–6].

By carefully choosing the conjugated polymer backbone or altering the side-chain functionalities, one should be able to fabricate EL devices in a variety of colors [7–9]. Many investigations have been focused on poly(*p*-phenylenevinylene)s (PPVs) since the discovery of EL in 1990 by a Cambridge group [10], and abundant derivatives of PPV have been reported with various substituents such as alkoxyl [11,12], silyl [13], phenyl [14], fluorenyl [15], halide [16–19], or cyano groups [8,20]. It has been possible to generate conjugated polymers with EL and photoluminescence (PL) across the full spectrum: red [21]; yellow-orange [22]; yellow [23]; yellow-green [24]; green [25]; and blue [26]. Conjugated polymers in general have a tendency to aggregate or stack as a consequence of their extensive π-delocalization. The solubility of the materials results from the presence of long alkyl chains that afford some conformational mobility to the polymer chains. Poly(2,5-dialkoxy-1,4-phenylenevinylene)s with long solubilizing alkoxy chains can be dissolved in conventional organic solvents such as chloroform, toluene, or tetrahydrofuran [27].

Through introduction of flexible side chains on the polymer backbone, one could achieve solubility and processability of aromatic conjugated polymers [28,29]. Flexible side chains also give rise to steric hindrance along the polymer backbone for the control of effective conjugation length and emission color of the polymers [30,31]. Control over materials morphology is an important matter in the properties of conjugated polymers which can exist in a large number of morphological organizations stemming from the interrelation between the polymers [32,33]. The structural flexibility of conjugated polymers generates highly disordered areas [34], while the rigidity of the aromatic segments promotes aggregate formation due to intermolecular interaction. Amorphous molecular materials, characterized by their high density of active units, good processability, transparency and homogeneous properties [35], can restrain molecular packing, extensive aggregation and morphological heterogeneity of conjugated polymers. Unfortunately, the rigid aromatic units have a strong tendency to form

---

* Corresponding author. Tel.: +82 51 510 2203; fax: +82 51 516 7421.
E-mail address: hssuh@pusan.ac.kr (H. Suh).

0032-3861/$ – see front matter Crown Copyright © 2008 Published by Elsevier Ltd. All rights reserved.
doi:10.1016/j.polymer.2008.08.037

interchain species such as aggregates or excimers. In comparison to emission from non-interacting chromophores, these ordered structures have red-shifted emission contributions and lower photoluminescent efficiencies [36]. A decrease in the efficiencies of PL and EL is often caused by the intermolecular interactions of such linear polymers [37,38].

The present investigation deals with the synthesis, characterization, photophysics, and EL of new polymers, poly[2-dimethyl(octyl)silyl-5-(4-(dimethyl(octyl)silyl)phenyl)-1,4-phenylenevinylene] (**P1**), poly[2,5-bis(4-(dimethyl(octyl)silyl)phenyl)-1,4-phenylenevinylene] (**P2**), poly[2,5-bis(9,9-dihexylfluorenyl)-1,4-phenylenevinylene] (**P3**), and poly[2,5-bis(4-(4-(2-etylhexyloxy)phenyl)phenyl)-1,4-phenylenevinylene] (**P4**), which were synthesized by Gilch polymerization. We previously reported the synthesis and EL properties of new PPVs, including poly[2-(2-ethylhexyloxy)-5-(4-(4-(2-ethylhexyloxy)phenyl)phenyl)-1,4-phenylenevinylene] (EEPP–PPV), poly[2,5-bis(4-(2-ethylhexyloxy)phenyl)-1,4-phenylenevinylene] (BEHP–PPV) and poly[2-(2-ethylhexyloxy)-5-(9,9-bis(2-etylhexyl)-fluorene-2-yl)-1,4-phenylenevinylene] (EHF–PPV) with terphenyl units, whose structures are shown in Fig. 1 [39]. **P1**–**P4** with various phenyl substituents, which induce intermolecular interaction in the solid state, achieve more blue-shifted absorption and emission peaks due to steric hindrance and apply to the color tuning and device performance improving of the conjugated polymer as the emissive layer in PLED. The results presented herein have broad implications for PPV with phenyl substituents being developed for application in PLEDs.

2. Experimental section

2.1. Materials and instruments

All reagents were purchased from Aldrich or TCI, and used without further purification. Solvents were purified by normal procedure and handled under moisture-free atmosphere. ^{1}H and ^{13}C NMR spectra were recorded with a Varian Gemini-200 (200 MHz), Unityplus-300 (300 MHz) and Inova-500 (500 MHz) spectrometer and chemical shifts were recorded in ppm units with TMS as the internal standard. Flash column chromatography was performed with Merck silica gel 60 (particle size 230–400 mesh ASTM) with ethyl acetate/hexane or methanol/methylene chloride gradients unless otherwise indicated. Analytical thin layer chromatography (TLC) was conducted using Merck 0.25 mm silica gel 60F pre-coated aluminum plates with fluorescent indicator UV254. UV spectra were recorded with a Varian 5E UV/vis spectrophotometer. The PL and EL spectra of the device were measured using an Oriel InstaSpec IV CCD detection systems in combination with a monochromatic light source. For PL spectrum measurements, xenon lamp was used as the excitation source, and incident beam took the maximum absorption peak of the polymers. Molecular weights and polydispersities of the polymers were determined by gel permeation chromatography (GPC) analysis with a polystyrene standard calibration. To examine electrochemical properties of the resulting polymer, the polymer film was cast from THF solution onto a platinum plate as a working electrode. Cyclic voltammetric waves were produced by using a EG&G Parc model 273 potentiostat/galvanostat at a constant scan rate of 100 mV/s. Elemental analysis (Korea Basic Science Institute: Daegu) was observed towards identification of the structure of polymers. “The spectra of FAB Mass” using at Korea Basic Science Institute Seoul Branch and Korea Basic Science Institute Daegu Branch.

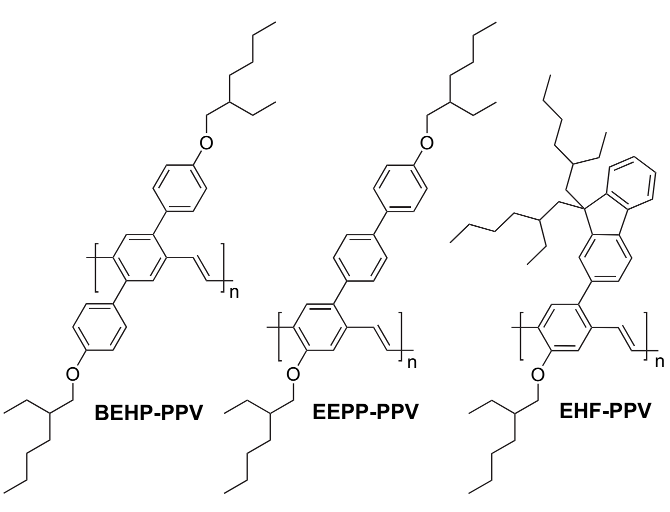

Fig. 1. Polymer structures of BEHP–PPV, EEPP–PPV and EHF–PPV with various terphenyl units.

2.2. EL device fabrication and measurements

For the EL experiment, poly(3,4-ethylenedioxythiophene) (PEDOT) doped with poly(styrenesulfonate) (PSS), as the hole-injection-transport layer, was introduced between emissive layer and ITO glass substrate cleaned by successive ultrasonic treatments. A solution of PEDOT/PSS in isopropanol was spin-coated on the surface-treated ITO substrate. On top of the PEDOT/PSS layer, the emissive polymer film was obtained by spin casting ODCB (*o*-dichlorobenzene) solution of the polymer. The emissive polymer thin film prepared had a uniform surface with a thickness of around 110 nm. The emissive film was dried in vacuum, and aluminum electrodes were deposited on the top of the polymer films through a mask by vacuum evaporation at pressures below 10^{-7} torr, yielding active areas of 4 mm^2. For the determination of device characteristics, current density–voltage (*J*–*V*) characteristics were measured using a Keithley 236 source measure unit. All processing steps and measurements mentioned above were carried out under air and at room temperature.

2.3. Synthesis of monomer and polymer

2.3.1. (4-Bromophenyl)(dimethyl)octylsilane (**1**)

To a stirred solution of 14.3 g (60.6 mmol) of 1,4-dibromobenzene in 150 mL of dry THF at −78 °C under argon atmosphere was added 37.8 mL (61 mmol) of *n*-BuLi (1.6 M *n*-hexane solution). After the addition of *n*-BuLi, the mixture was stirred at −78 °C for 2 h. To the reaction mixture, 12.5 g (60.6 mmol) of dimethyl-*n*-octylchlorosilane was added dropwise at −78 °C. The solution was allowed to warm to room temperature and stirred for an additional 3 h. The reaction mixture was concentrated under reduced pressure, and purified by flash column chromatography (60 × 300 mm column, SiO$_2$, 100% hexane) to give 15 g (75.6%) of compound **1**, yellow oil: R_f 0.91 (SiO$_2$, hexane 100%).

^{1}H NMR (200 MHz, CDCl$_3$): δ (ppm) 7.49–7.45 (d, 2H), 7.36–7.32 (d, 2H), 1.35–1.15 (m, 12H), 0.87–0.83 (m, 3H), 0.76–0.70 (m, 2H), 0.22 (s, 6H); ^{13}C NMR (75 MHz, CDCl$_3$): δ (ppm) 138.77, 135.42, 131.09, 123.78, 33.81, 32.19, 29.52, 24.05, 22.94, 15.83, 14.38, −2.82; HRMS (EI) *m*/*z* 326.1060 (calculated for $C_{16}H_{27}BrSi$ 326.1065).

2.3.2. (4-Bromo-2,5-dimethylphenyl)(dimethyl)octylsilane (**2**)

To a stirred solution of 31.94 g (121 mmol) of 2,5-dibromo-*p*-xylene in 200 mL of dry THF at −78 °C under argon atmosphere was added 75.6 mL (121 mmol) of *n*-BuLi (1.6 M *n*-hexane solution). After the addition of *n*-BuLi, the mixture was stirred at −78 °C for 2 h. To the reaction mixture, 25 g (121 mmol) of dimethyl-*n*-octylchlorosilane was added dropwise at −78 °C. The solution was allowed to warm to room temperature and stirred for an additional

3 h. The reaction mixture was concentrated under reduced pressure, and purified by flash column chromatography (60 × 300 mm column, SiO_2, 100% hexane) to give 35 g (81%) of compound **2**, yellow oil: R_f 0.93 (SiO_2, hexane 100%).

^{1}H NMR (200 MHz, $CDCl_3$): δ (ppm) 7.40 (s, 1H), 7.34 (s, 1H), 2.39 (s, 3H), 2.37 (s, 3H), 1.29–1.26 (m, 12H), 0.98–0.80 (m, 5H), 0.30 (s, 6H); ^{13}C NMR (75 MHz, $CDCl_3$): δ (ppm) 142.94, 137.18, 137.15, 134.12, 133.59, 126.38, 33.87, 32.22, 29.56, 24.27, 22.99, 22.58, 22.39, 16.24, 14.40, −1.64; HRMS (EI) m/z 354.1377 (calculated for $C_{18}H_{31}BrSi$ 354.1378).

2.3.3. *4,4′-Bis[dimethyl(octyl)silyl]-2,5-dimethyl-1,1′-biphenyl (**3**)*

To a stirred suspension of 0.38 g (15.5 mmol) of magnesium in 30 mL ether under argon atmosphere was added slowly 5.1 g (15.5 mmol) of (4-bromophenyl)(dimethyl)octylsilane (**1**) over 5 min. The mixture was stirred at 50 °C for 3 h and cooled down. The clear solution was added into a mixture of 5.5 g (15.5 mmol) of (4-bromo-2,5-dimethylphenyl)(dimethyl)octylsilane (**2**) and 59 mg (0.108 mmol) of $Ni(dppp)_2Cl_2$ in 30 mL ether under an inert atmosphere (Ar) and was refluxed for 18 h. After the reaction was completed, the mixture was poured into water and extracted by ether. The organic layer was washed by Na_2CO_3 and NaCl aqueous solutions, respectively, and dried with $MgSO_4$. After removal of the solvent (ether) the residue was purified by flash chromatography (40 × 300 mm column, SiO_2, 100% hexane) to give 2.77 g (34.2%) of title compound **3**: R_f 0.65 (SiO_2, hexane 100%).

^{1}H NMR (200 MHz, $CDCl_3$): δ (ppm) 7.57–7.50 (m, 2H), 7.41 (s, 1H), 7.32–7.25 (m, 2H), 7.03 (s, 1H), 2.41 (s, 3H), 2.25 (s, 3H). 1.29–1.24 (m, 24H), 0.86–0.79 (m, 10H), 0.27 (s, 6H), 0.23 (s, 6H); ^{13}C NMR (75 MHz, $CDCl_3$): δ (ppm) 142.63, 141.43, 135.38, 134.31, 133.65, 132.82, 128.98, 127.48, 127.40, 126.68, 32.27, 32.25, 31.14, 31.11, 29.66, 29.60, 28.68, 28.65, 22.91, 22.90, 20.22, 20.15, 18.95, 17.89, 16.03, 15.99, 14.39, 14.35, −2.66, −2.69; HRMS (EI) m/z 522.4082 (calculated for $C_{34}H_{58}Si_2$ 522.4077).

2.3.4. *2,5-Bis(bromomethyl)-4,4′-bis[dimethyl(octyl)silyl]-1,1′-biphenyl (**4**)*

To a stirred solution of 2.8 g (5.4 mmol) of 4,4′-bis[dimethyl(octyl)silyl]-2,5-dimethyl-1,1′-biphenyl (**3**), and 1.89 g (110 mmol) of NBS in 200 mL of CCl_4 at room temperature was emitted the light source (300 W) for 1 h. The reaction mixture was filtered in order to remove succinimide, concentrated *in vacuo*, and purified by column chromatography (40 × 300 mm column, SiO_2, 100% hexane) to provide 1.21 g (33%) of the desired final brominated product **4**: R_f 0.71 (SiO_2, hexane 100%).

^{1}H NMR (200 MHz, $CDCl_3$): δ (ppm) 7.59–7.56 (d, 2H), 7.44–7.40 (d, 2H), 7.34 (s, 2H), 4.59 (s, 2H), 4.46 (s, 2H), 1.30–0.83 (m, 34H), 0.40 (s, 6H), 0.28 (s, 6H); ^{13}C NMR (75 MHz, $CDCl_3$): δ (ppm) 142.57, 141.63, 135.23, 133.91, 133.15, 132.92, 128.77, 128.01, 127.44, 126.53, 33.84, 32.72, 32.12, 32.09, 31.23, 31.20, 29.28, 29.23, 28.34, 28.31, 23.12, 23.09, 20.92, 20.87, 16.47, 16.39, 14.77, 14.71, −2.63, −2.68; HRMS (EI) m/z 680.2269 (calculated for $C_{34}H_{56}Br_2Si_2$ 680.2267).

2.3.5. *Dimethyl(octyl)[4-(4,4,5,5-tetramethyl-1,3,2-dioxaborolan-2-yl)phenyl]silane (**5**)*

To a stirred solution of 5 g (15.3 mmol) of (4-bromophenyl)(dimethyl)octylsilane (**1**) in 100 mL of dry THF at −78 °C under argon atmosphere was added 9.6 mL (15.3 mmol) of *n*-BuLi (1.6 M *n*-hexane solution). After the addition of *n*-BuLi, the mixture was stirred at −78 °C for 2 h. To the reaction mixture, 4.7 mL (23 mmol) of 2-isopropoxy-4,4,5,5-tetramethyl-1,3,2-dioxaborolane was added dropwise at −78 °C. The solution was allowed to warm to room temperature and stirred for an additional 3 h. The reaction mixture was quenched by HCl (1 N) solution and water, and extracted with ether. The organic phase was concentrated under reduced pressure, and purified by flash column chromatography (30 × 300 mm column, SiO_2, 100% hexane) to give 4.12 g (72%) of compound **5**: R_f 0.26 (SiO_2, hexane 100%).

^{1}H NMR (200 MHz, $CDCl_3$): δ (ppm) 7.79 (d, 2H), 7.52 (d, 2H), 1.33 (s, 12H) 1.22 (s, 12H), 0.88–0.82 (m, 5H), 0.24 (s, 6H); HRMS (EI) m/z 374.2819 (calculated for $C_{22}H_{39}BO_2Si$ 374.2812).

2.3.6. *4,4″-Bis[dimethyl(octyl)silyl]-2′,5′-dimethyl-[1,1′,4′,1″]terphenyl (**6**)*

To a stirred solution of 4.12 g (11 mmol) of borolane compound **5** in 100 mL of toluene, 50 mL of ethyl alcohol, and 50 mL of aqueous Na_2CO_3 (2 M) was added 1.45 g (5.5 mmol) of 2,5-dibromo-*p*-xylene. After the solution was purged with nitrogen for 20 min, 1.27 g (1.1 mmol) of tetrakis(triphenylphosphine)palladium(0) ($Pd[P(Ph)_3]_4$) was added. The reaction mixture was refluxed with vigorous stirring under nitrogen for 24 h. The reaction mixture was diluted with ethyl acetate and water. The organic phase was separated and washed with brine and dried over $MgSO_4$. The crude product was purified by column chromatography (30 × 300 mm column, SiO_2, 100% hexane) to give 2.7 g (81%) of compound **6**: R_f 0.43 (SiO_2, hexane 100%).

^{1}H NMR (200 MHz, $CDCl_3$): δ (ppm) 7.57–7.54 (d, 4H), 7.37–7.33 (d, 4H), 7.15 (s, 2H), 2.28 (s, 6H), 1.31–1.25 (m, 24H). 0.90–0.77 (m, 10H), 0.23 (s, 12H); ^{13}C NMR (75 MHz, $CDCl_3$): δ (ppm) 142.25, 141.01, 138.16, 133.57, 128.98, 128.76, 127.39, 33.87, 32.18, 29.52, 24.15, 22.92, 20.19, 16.02, 14.36, −2.67; HRMS (EI) m/z 598.4390 (calculated for $C_{40}H_{62}Si_2$ 598.4390).

2.3.7. *2′,5′-Bis-bromomethyl-4,4″-bis-(dimethyl(octyl)silyl)-[1,1′;4′,1″]terphenyl (**7**)*

To a stirred solution of 0.7 g (1.17 mmol) of compound **6**, and 0.42 g (2.35 mmol) of NBS in 200 mL of CCl_4 at room temperature was emitted the light source (300 W) for 1 h. The reaction mixture was filtered in order to remove succinimide, concentrated *in vacuo*, and purified by column chromatography (30 × 300 mm column, SiO_2, 100% hexane) to provide 0.18 g (mmol) of the desired final brominated product **7**: R_f 0.52 (SiO_2, hexane 100%).

^{1}H NMR (200 MHz, $CDCl_3$): δ (ppm) 7.65–7.58 (d, 4H), 7.55–7.45 (m, 6H), 4.42 (s, 4H), 1.51–1.18 (m, 24H), 0.92–0.72 (m, 10H), 0.32 (s, 12H); ^{13}C NMR (75 MHz, $CDCl_3$): δ (ppm) 142.38, 141.23, 137.98, 133.63, 129.11, 128.48, 127.37, 33.18, 32.26, 32.16, 29.73, 24.37, 23.03, 15.89, 14.35, −2.65; HRMS (EI) m/z 756.2585 (calculated for $C_{40}H_{60}Br_2Si_2$ 756.2580).

2.3.8. *2-Bromo-9,9-dihexyl-9H-fluorene (**8**)*

To a stirred solution of 10 g (40.8 mmol) of 2-bromo-9*H*-fluorene and catalytic amounts of triethylbenzylammonium chloride in 200 mL of DMSO under nitrogen was added 11.45 mL (81.6 mmol) of hexylbromide. After 1 h at 60 °C, 10 mL of 50% aqueous NaOH was added. The reaction mixture was cooled to room temperature and stirred for 5 h. An excess amount of ethyl acetate was added to the reaction mixture to generate the precipitate NaOH. After filtering off the precipitated NaOH, the organic layer was washed with 4 × 200 mL of water. The organic phase was dried with $MgSO_4$ and concentrated under reduced pressure. The residue was purified by flash column chromatography (60 × 300 mm column, SiO_2, hexane 100%) to give 14.99 g (89%) of extremely clean compound **8**, yellow oil: R_f 0.6 (SiO_2, hexane 100%).

^{1}H NMR (200 MHz, $CDCl_3$): δ (ppm) 7.66 (m, 2H), 7.57 (d, 1H, $J = 1.10$ Hz), 7.53 (s, 1H), 7.33 (m, 2H), 7.25 (d, 1H, $J = 1.10$ Hz), 1.09 (t, 4H, $J = 8.06$ Hz), 1.04 (m, 16H), 0.76 (t, 6H, $J = 6.96$ Hz); ^{13}C NMR (75 MHz, $CDCl_3$): δ (ppm) 153.24, 150.56, 140.43, 140.31, 130.18, 127.74, 127.21, 126.42, 123.12, 121.28, 120.12, 55.65, 40.60, 31.76, 29.94, 23.96, 22.86, 14.28; HRMS (EI) m/z 412.1768 (calculated for $C_{25}H_{33}Br$ 412.1766).

2.3.9. 9,9-Dihexyl-9H-fluoren-2-ylboronic acid (**9**)

To a stirred solution of 9.8 g (23.7 mmol) of 2-bromo-9,9-dihexyl-9*H*-fluorene (**8**) in 100 mL of dry THF at −78 °C under argon atmosphere was added 17.78 mL (28.45 mmol) of *n*-BuLi (1.6 M *n*-hexane solution). After the addition of *n*-BuLi, the mixture was stirred at −78 °C for 2 h. To the reaction mixture, 2.83 mL (24.89 mmol) of trimethoxy borate was added dropwise at −78 °C. The solution was allowed to warm to room temperature and stirred for an additional 3 h. The reaction mixture was quenched by HCl (1 N) solution and water, and extracted with ether. The organic phase was concentrated under reduced pressure, and purified by flash column chromatography (40 × 300 mm column, SiO_2, EA:hexane = 1:4) to give 5.8 g (64.7%) of compound **9**: R_f 0.11 (SiO_2, EA:hexane = 1:5).

^{1}H NMR (200 MHz, $CDCl_3$): δ (ppm) 8.32 (d, 1H, $J = 7.69$ Hz), 8.23 (s, 1H), 7.9 (d, 1H, $J = 7.69$ Hz), 7.82 (m, 2H), 7.40 (m, 2H), 2.08 (t, 4H, $J = 8.05$ Hz), 1.08 (m, 16H), 0.75 (t, 6H, $J = 6.23$ Hz); HRMS (EI) *m*/*z* 378.2734 (calculated for $C_{25}H_{35}BO_2$ 378.2730).

2.3.10. 2-[4-(9,9-Dihexyl-9H-fluoren-2-yl)-2,5-dimethylphenyl]-9,9-dihexyl-9H-fluorene (**10**)

To a stirred solution of 5 g (13.22 mmol) of 9,9-dihexyl-9*H*-fluoren-2-ylboronic acid in 100 mL of DME, 50 mL of ethyl alcohol, and 50 mL of aqueous Na_2CO_3 (2 M) was added 1.75 g (6.61 mmol) of 2,5-dibromo-*p*-xylene. After the solution was purged with nitrogen for 20 min, 1.53 g (1.32 mmol) of tetrakis (triphenylphosphine)palladium(0) ($Pd(PPh_3)_4$) was added. The reaction mixture was refluxed with vigorous stirring under nitrogen for 24 h. The reaction mixture was diluted with ethyl acetate and water. The organic phase was separated and washed with brine and dried over $MgSO_4$. The crude product was purified by column chromatography (30 × 300 mm column, SiO_2, methylene chloride:hexane = 1:9) to give 3 g (59%) of compound **10**: R_f 0.56 (SiO_2, methylene chloride:hexane = 1:5).

^{1}H NMR (200 MHz, $CDCl_3$): δ (ppm) 7.78 (d, 2H, $J = 5.13$ Hz), 7.74 (d, 2H, $J = 5.86$ Hz), 7.36 (m, 10H), 7.29 (s, 2H), 2.35 (s, 6H), 2.00 (m, 8H), 1.13 (m, 32H), 0.78 (t, 12H, $J = 6.59$ Hz); ^{13}C NMR (75 MHz, $CDCl_3$): δ (ppm) 151.41, 150.72, 142.65, 140.87, 139.86, 138.67, 135.84, 133.79, 127.70, 127.51, 126.76, 124.02, 123.64, 119.40, 119.27, 55.17, 40.55, 31.32, 29.66, 24.06, 22.80, 16.20, 14.05; HRMS (EI) *m*/*z* 770.5797 (calculated for $C_{58}H_{74}$ 770.5791).

2.3.11. 2-[2,5-Bis(bromomethyl)-4-(9,9-dihexyl-9H-fluoren-2-yl)phenyl]-9,9-dihexy-9H-fluorene (**11**)

To a stirred solution of 1.6 g (2.1 mmol) of compound **10**, and 0.75 g (4.2 mmol) of NBS in 200 mL of CCl_4 at room temperature was emitted the light source (300 W) for 1 h. The reaction mixture was filtered in order to remove succinimide, concentrated *in vacuo*, and purified by column chromatography (30 × 300 mm column, SiO_2, methylene chloride:hexane = 1:9) to provide 0.5 g (25.6%) of the desired final brominated product **7**: R_f 0.42 (SiO_2, methylene chloride:hexane = 1:5).

^{1}H NMR (200 MHz, $CDCl_3$): δ (ppm) 7.80 (d, 2H, $J = 8.43$ Hz), 7.76 (d, 2H, $J = 7.69$ Hz), 7.56 (d, 4H, $J = 5.86$ Hz), 7.42 (d, 2H, $J = 8.79$ Hz), 7.36 (m, 6H), 4.50 (s, 4H), 2.20 (m, 8H), 1.10 (m, 32H), 0.73 (t, 12H, $J = 7.33$ Hz); ^{13}C NMR (75 MHz, $CDCl_3$): δ (ppm) 151.28, 151.21, 142.54, 141.03, 140.87, 138.13, 135.97, 133.21, 127.92, 127.53, 127.08, 123.76, 123.17, 120.08, 119,90, 55.49, 40.69, 31.89, 31.77, 29.94, 24.08, 22.81, 14.24; HRMS (FAB) *m*/*z* 926.3995 (calculated for $C_{58}H_{72}Br_2$ 926.4001).

2.3.12. 4-Bromo-4′-[(2-ethylhexyl)oxy]-1,1′-biphenyl (**12**)

To a stirred solution of 10 g (40.14 mmol) of 4-bromo-4-hydroxy biphenyl, 3.18 g (48.17 mmol) of potassium hydroxide and 0.6 g (4.08 mmol) of sodium iodide in 150 mL of ethyl alcohol at room temperature under argon atmosphere was added 11.16 mL (60.22 mmol) of 2-ethylhexyl bromide. After being refluxed for 3 days, the reaction mixture was cooled and filtered. The mixture was concentrated *in vacuo*, diluted with ethyl acetate, and washed with 2 times of 30 mL of water and 30 mL of saturated sodium chloride solution. The obtained crude product was recrystallized with MeOH to provide 9.71 g (67%) of the desired product **12**: R_f 0.4 (SiO_2, hexane 100%).

^{1}H NMR (200 MHz, $CDCl_3$) δ (ppm) 7.52 (d, 2H, $J = 8.0$ Hz), 7.47 (d, 2H, $J = 8.8$ Hz), 7.40 (d, 2H, $J = 8.0$ Hz), 6.96 (d, 2H, $J = 8.8$ Hz), 3.87 (d, 2H, $J = 5.5$ Hz), 0.81–1.64 (m, 15H); ^{13}C NMR (50 MHz, $CDCl_3$) δ (ppm) 157.51, 142.39, 131.98, 130.93, 128.50, 128.13, 115.15, 112.26, 70.86, 39.61, 30.75, 29.31, 24.10, 23.27, 14.29, 11.32; HRMS (EI) *m*/*z* 360.1098 (calculated for $C_{20}H_{25}BrO$ 360.1089).

2.3.13. 2-[4-[(2-Ethylhexyl)oxy][1,1-biphenyl]-4-yl]-4,4,5,5-tetramethyl-1,3,2-dioxaborolane (**13**)

To a stirred solution of 5 g (13.8 mmol) of 4-bromo-4-[(2-etylhexyl)oxy]-1,1-biphenyl (**12**) in dry THF (50 mL) at −78 °C under argon atmosphere was added 10.4 mL (16 mmol) of *n*-BuLi (1.6 M *n*-hexane solution). After stirring for 2 h at −78 °C, the reaction mixture was treated with 3.38 mL of (16.6 mmol) of 2-isopropoxy-4,4,5,5-tetramethyl-1,3,2-dioxaborolan −78 °C. The solution was allowed to warm to room temperature and stirred for an additional 3 h. The reaction mixture was quenched by water, and extracted with 250 mL of ether. After removing the solvent under reduced pressure, the yellow residue was purified by column chromatography to provide 4.6 g (82%) of the desired final borolane product **13** as yellow oil: R_f 0.3 (SiO_2, hexane 100%).

^{1}H NMR (200 MHz, $CDCl_3$) δ (ppm) 7.86 (d, 2H, $J = 8.1$ Hz), 7.57 (d, 2H, $J = 8.4$ Hz), 7.55 (d, 2H, $J = 8.8$ Hz), 6.97 (d, 2H, $J = 8.8$ Hz), 3.88 (d, 2H, $J = 5.5$ Hz), 1.74 (m, 1H), 1.32 (s, 12H), 1.22–1.53 (m, 8H), 0.90–0.97 (s, 6H); ^{13}C NMR (75 MHz, $CDCl_3$) δ (ppm) 159.28, 143.60, 135.26, 133.21, 128.18, 125.96, 114.84, 83.75, 70.61, 39.42, 30.56, 29.10, 24.88, 23.90, 23.07, 14.09, 11.13; HRMS (EI) *m*/*z* 408.2839 (calculated for $C_{26}H_{37}BO_3$ 408.2836).

2.3.14. 4,4⁗-Bis-(2-ethyl-hexyloxy)-2″,5″-dimethyl-[1,4′;1′,1″;4″,1‴;4‴,1⁗]quinquephenyl (**14**)

To a stirred solution of 11.87 g (29.06 mmol) of compound **13** in 100 mL of DME, 50 mL of ethyl alcohol, and 50 mL of aqueous Na_2CO_3 (2 M) was added 2.64 g (10 mmol) of 2,5-dibromo-*p*-xylene. After the solution was purged with nitrogen for 20 min, 3.36 g (2.91 mmol) of tetrakis(triphenylphosphine)palladium(0) ($Pd(PPh_3)_4$) was added. The reaction mixture was refluxed with vigorous stirring under nitrogen for 24 h. The reaction mixture was diluted with ethyl acetate and water. The organic phase was separated and washed with brine and dried over $MgSO_4$. The crude product was purified by column chromatography (60 × 300 mm column, SiO_2, EA:hexane = 1:10) to give 3.58 g (53.7%) of compound **14**: R_f 0.53 (SiO_2, EA:hexane = 1:10).

^{1}H NMR (200 MHz, $CDCl_3$): δ (ppm) 7.62 (d, 4H, $J = 8.06$ Hz), 7.56 (s, 2H), 7.43 (d, 4H, $J = 8.06$ Hz), 7.24 (d, 4H, $J = 8.06$ Hz), 7.00 (d, 4H, $J = 8.43$ Hz), 3.90 (d, 4H, $J = 5.49$ Hz), 2.34 (s, 6H), 1.76 (m, 2H), 1.45 (m, 16H), 0.95 (t, 12H, $J = 7.14$ Hz); 157.84, 142.72, 131.89, 131.23, 130.84, 128.74, 128.52, 127.21, 126.91, 115.62, 113.87, 70.83, 39.73, 30.77, 29.39, 24.26, 23.36, 17.86, 14.40, 11.39; HRMS (EI) *m*/*z* 666.4441 (calculated for $C_{48}H_{58}O_2$ 666.4437).

2.3.15. 2″,5″-Bis-bromomethyl-4,4⁗-bis-(2-ethyl-hexyloxy)-[1,4′;1′,1″;4″,1‴;4‴,1⁗]quinquephenyl (**15**)

To a stirred solution of 3.2 g (4.8 mmol) of compound **14**, and 2.05 g (11.52 mmol) of NBS in 200 mL of CCl_4 at room temperature was emitted the light source (300 W) for 1 h. The reaction mixture was filtered in order to remove succinimide, concentrated *in vacuo*, and purified by column chromatography (30 × 300 mm column, SiO_2, EA:hexane = 1:10) to provide 2.1 g (53%) of the desired final brominated product **15**: R_f 0.59 (SiO_2, EA:hexane = 1:10).

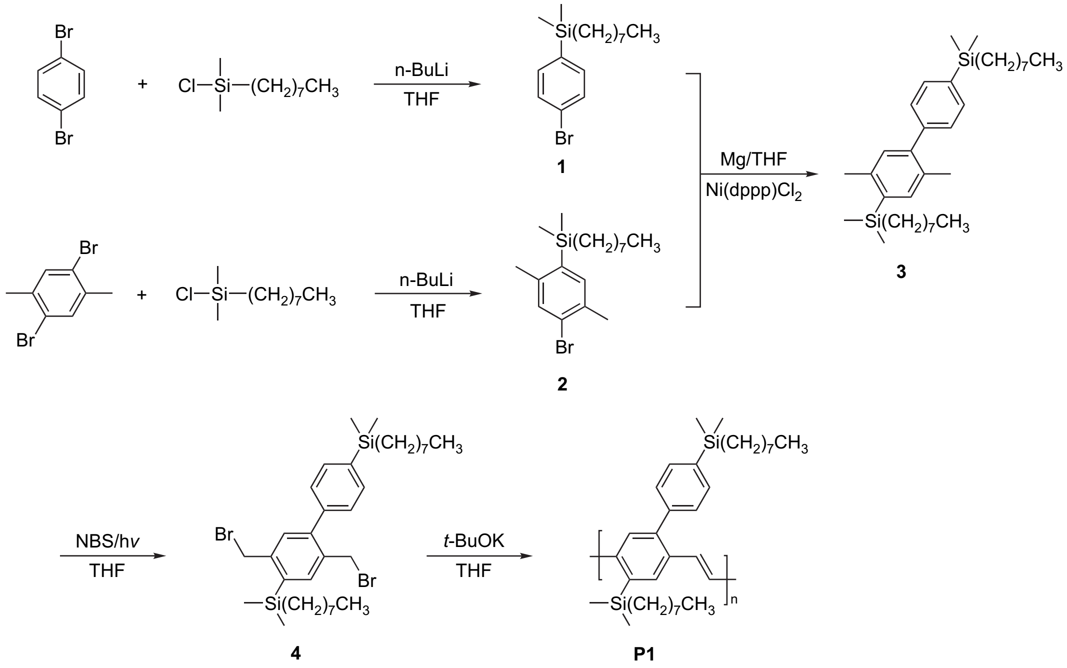

Scheme 1. Synthetic route for the monomer and the polymer, **P1**.

^{1}H NMR (200 MHz, CDCl$_3$): δ (ppm) 7.60 (m, 14H), 7.02 (d, 4H, $J = 8.79$ Hz), 4.53 (s, 4H), 3.91 (d, 4H, $J = 5.86$ Hz), 1.76 (m, 2H), 1.4 (m, 16H), 0.92 (m, 12H); 157.61, 142.42, 133.07, 131.87, 130.91, 128.47, 128.25, 127.07, 126.85, 115.48, 113.64, 70.81, 39.66, 32.78, 30.74, 29.37, 24.20, 23.31, 14.35, 11.37; HRMS (EI) m/z 822.2641 (calculated for $C_{48}H_{56}Br_2O_2$ 822.2647).

2.3.16. *Polymers (**P1**, **P2**, **P3**, and **P4**)*

To a stirred solution of the 1 mmol of monomer **4**, **7**, **11**, and **15** in 50 mL of dry THF, 6 mL of the potassium *tert*-butoxide (1.0 M THF solution, 6 mmol) was added drop-wise for 2 h by a syringe pump at 30 °C. During this addition, the reaction mixture had color change from colorless to green, and the viscosity increased significantly. After the addition was complete, the reaction mixture was stirred additionally for 12 h at 30 °C. The polymerization solution was poured into 500 mL of methanol with stirring. The precipitated polymer was filtered off, and the resulting polymer was dissolved again in THF. The dissolving polymer was slowly poured into 500 mL of intensively stirred methanol. The precipitated polymer was filtered off, washed with water, and dried under reduced pressure at room temperature. 200–400 mg samples of polymers were obtained as green or yellow fibers.

3. Results and discussion

3.1. *Synthesis and characterization*

The general synthetic routes toward the monomers and polymers are outlined in Schemes 1, 2 and 3. For the preparation of **P1**, as shown in Scheme 1, in the first step, the commercially available 1,4-dibromobenzene was chosen as the starting material and coupled with dimethyl-*n*-octylchlorosilane using *n*-butyl lithium (*n*-BuLi) in

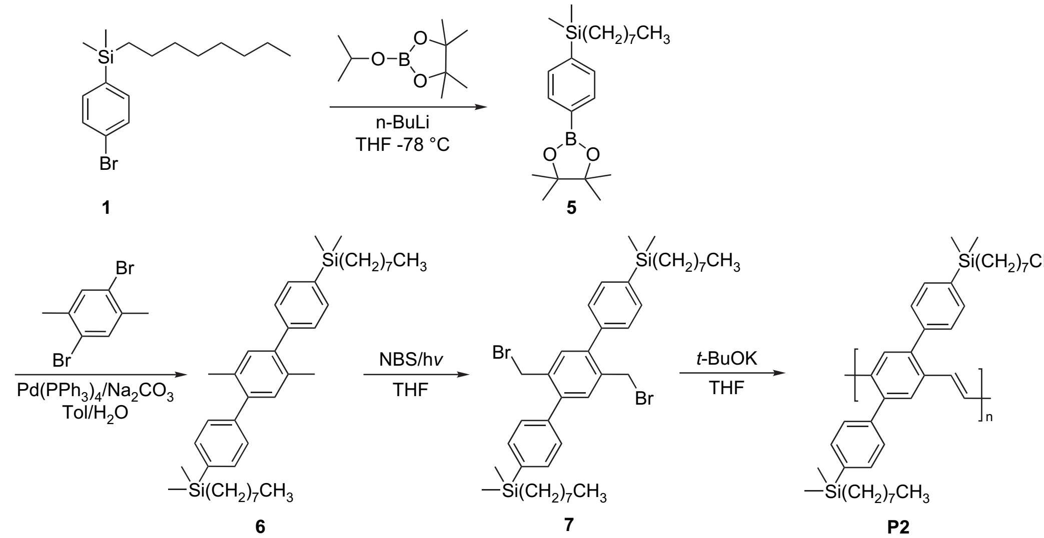

Scheme 2. Synthetic route for the monomer and the polymer, **P2**.

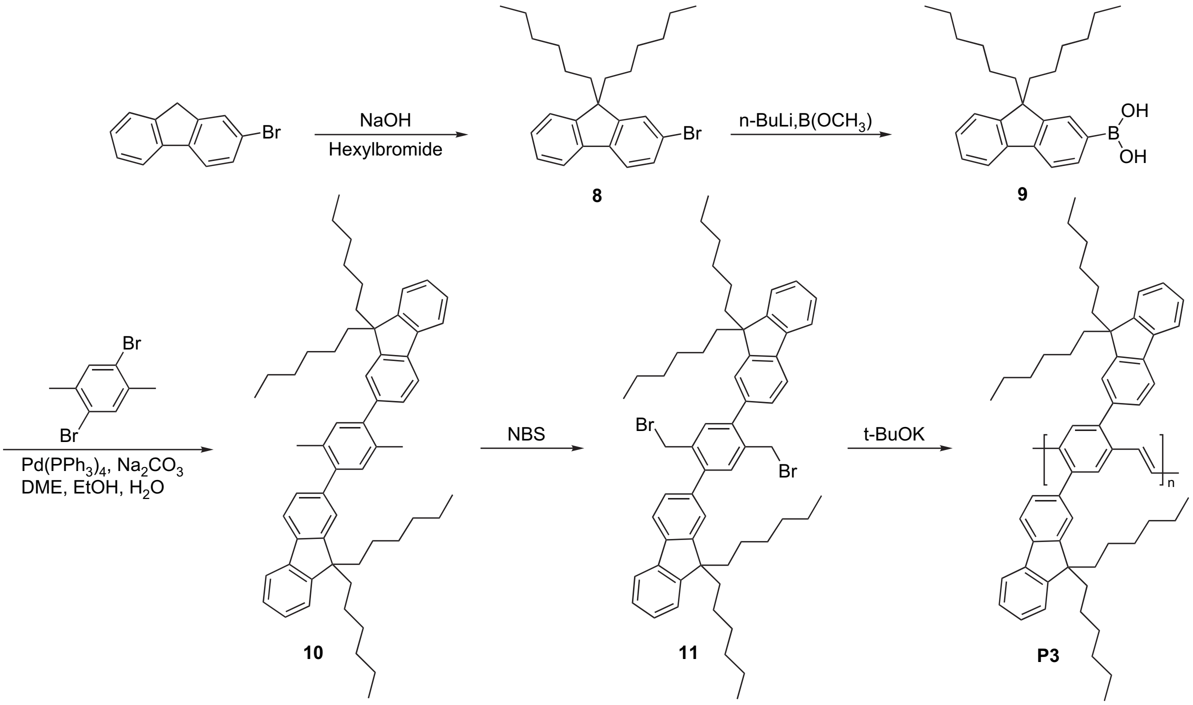

Scheme 3. Synthetic route for the monomer and the polymer, **P3**.

THF at −78 °C to produce (4-bromophenyl)(dimethyl)octylsilane (**1**). Another commercially available material, 2,5-dibromo-*p*-xylene, was also coupled with dimethyl-*n*-octylchlorosilane using *n*-BuLi in THF at −78 °C to produce (4-bromo-2,5-dimethylphenyl)(dimethyl)octylsilane (**2**). The resulting compounds, **1** and **2**, were coupled with nickel catalyst and Mg in ether. This coupled 4,4′-bis[dimethyl(octyl)silyl]-2,5-dimethyl-1,1′-biphenyl (**3**) was brominated at the benzyl positions with NBS and a light source (300 W) in CCl_4 to generate monomer **4**. In order to synthesize **P2**, as shown in Scheme 2, the previously prepared compound **1** was treated with 2-isopropoxy-4,4,5,5-tetramethyl-1,3,2-dioxaborolane and *n*-butyl lithium in THF to generate borolane compound **5**, which

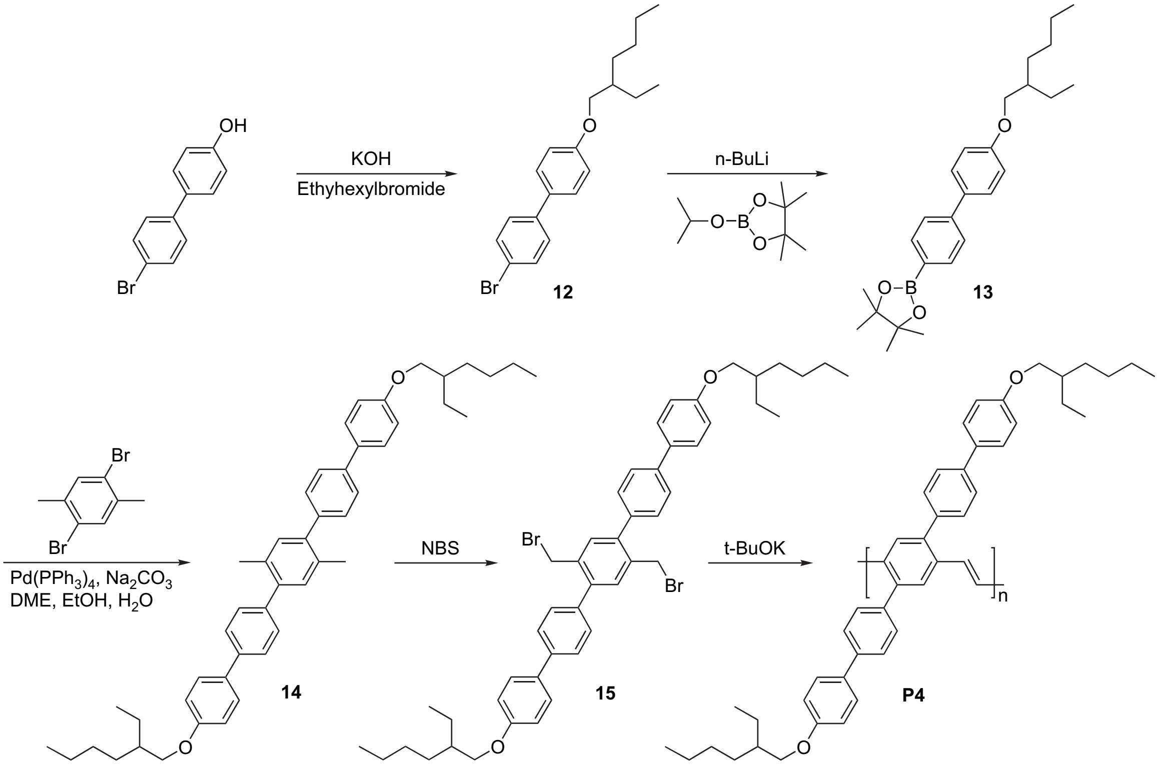

Scheme 4. Synthetic route for the monomer and the polymer, **P4**.

Table 1
Results of polymerization

Polymer	Substituents	M_n[a] ($\times 10^3$)	M_w[a] ($\times 10^3$)	PDI[a]	T_g[b] (°C)	T_d[c] (°C)
P1	Silyl and silylphenyl groups	30	63	2.1	115	400
P2	Bis-silylphenyl groups	47	122	2.6	144	415
P3	Bis-fluorene groups	9	29	3.2	141	423
P4	Bis-diphenyl groups	41	98	2.4	127	408

[a] Molecular weight (M_w) and polydispersity (PDI) of the polymers were determined by gel permeation chromatography (GPC) in THF using polystyrene standards.
[b] Glass transition temperature measured by DSC under N_2.
[c] Onset decomposition temperature (5% weight loss) measured by TGA under N_2.

was coupled with 2,5-dibromo-*p*-xylene using tetrakis(triphenylphosphine)palladium catalyst and sodium carbonate in toluene and water by Suzuki coupling. This coupled 4,4″-bis[dimethyl(octyl)silyl]-2′,5′-dimethyl-[1,1′,4′,1″]terphenyl (**6**) was brominated at the benzyl positions with NBS and a light source (300 W) in CCl_4 to generate monomer **7**. For the preparation of **P3**, as shown in Scheme 3, the commercially available 2-bromo-9H-fluorene was chosen as the starting material and coupled with hexylbromide using sodium hydroxide and tetra-*n*-butyl ammonium bromide as a phase transfer catalyst in DMSO. The resulting compound **8** was treated with trimethoxy borate and *n*-butyl lithium in THF to generate boronic acid compound **9**, which was coupled with 2,5-dibromo-*p*-xylene using tetrakis(triphenylphosphine)palladium catalyst and sodium carbonate in DME and water by Suzuki coupling. This coupled 2-[4-(9,9-dihexyl-9*H*-fluoren-2-yl)-2,5-dimethylphenyl]-9,9-dihexyl-9*H*-fluorene (**10**) was brominated at the benzyl positions with NBS and a light source (300 W) in CCl_4 to generate monomer **11**. In order to synthesize **P4**, as shown in Scheme 4, the commercially available 4-bromo-4′-hydroxybiphenyl was coupled with 2-ethylhexyl bromide using potassium hydroxide in ethyl alcohol to provide 4-bromo-4′-[(2-ethylhexyl)oxy]-1,1′-biphenyl (**12**). Compound **12** was coupled with 2-isopropoxy-4,4,5,5-tetramethyl-1,3,2-dioxaborolane using *n*-butyl lithium in THF to generate borolane compound **13**, which was coupled with 2,5-dibromo-*p*-xylene using tetrakis(triphenylphosphine)palladium catalyst and sodium carbonate in DME and water by Suzuki coupling. This coupled compound **14** was brominated at the benzyl positions with NBS and a light source (300 W) in CCl_4 to generate monomer **15**. The polymers (**P1**, **P2**, **P3**, and **P4**) were prepared by the Gilch reaction, using monomers (**4**, **7**, **11**, and **15**) and an excess amount of potassium *tert*-butoxide in THF at 30 °C for 24 h under argon atmosphere.

The resulting polymers were soluble in organic solvents such as chloroform, tetrahydrofuran, dichloromethane, and chlorobenzene. The number-average molecular weight (M_n) and the weight-average molecular weight (M_w) of polymers were 9,000–47,000 and 29,000–122,000 with a polydispersity between 2.1 and 3.2 as determined by GPC using THF as the eluant and polystyrene as the standard (Table 1). The thermal properties of the polymers were determined by DSC and thermal gravimetric analysis under a nitrogen atmosphere at a heating rate of 10 °C/min. Polymers showed glass transitions at 100–141 °C and loses less than 5% of their weights on heating to 400–423 °C. These T_g and T_d were higher than those of other conjugated polymers. The high thermal stability of the resulting polymer prevented the deformation of the polymer morphology and degradation of the polymer light-emitting device by applied electric field of the LED.

Table 2
Optical properties of polymers

Polymers	In solution (nm)			In film (nm)		
	Abs λ_{max}	PL λ_{max}[a]	fwhm[b]	Abs λ_{max}	PL λ_{max}[a]	fwhm[b]
P1	423	495	61	419	549 (521)	109
P2	388	482	75	404	537 (510)	104
P3	413	485	69	425	521	100
P4	409	503	67	418	543	105

[a] The data in the parentheses are the wavelengths of shoulders and subpeaks.
[b] Full width at half-maximum of the PL spectra.

3.2. Absorption and photoluminescence properties of polymer

The optical absorption and photoluminescence (PL) properties of the polymers were investigated both in THF solutions and thin solid films. The concentrations of all the THF solutions were fixed at 1×10^{-5} M. Transparent and uniform polymer films were prepared on quartz plates by spin-casting from their respective *o*-dichlorobenzene (ODCB) solution at room temperature. The absorption and emission data for the polymers are summarized in Table 2. There is little difference between the absorption and emission spectra of the polymers in the solutions and the thin films, which can be attributed to the π–π* transitions of the polymers.

The optical spectra of **P1** and **P2** are shown in Fig. 2. The absorption spectrum of **P1** and **P2** exhibited maximum peak at 423

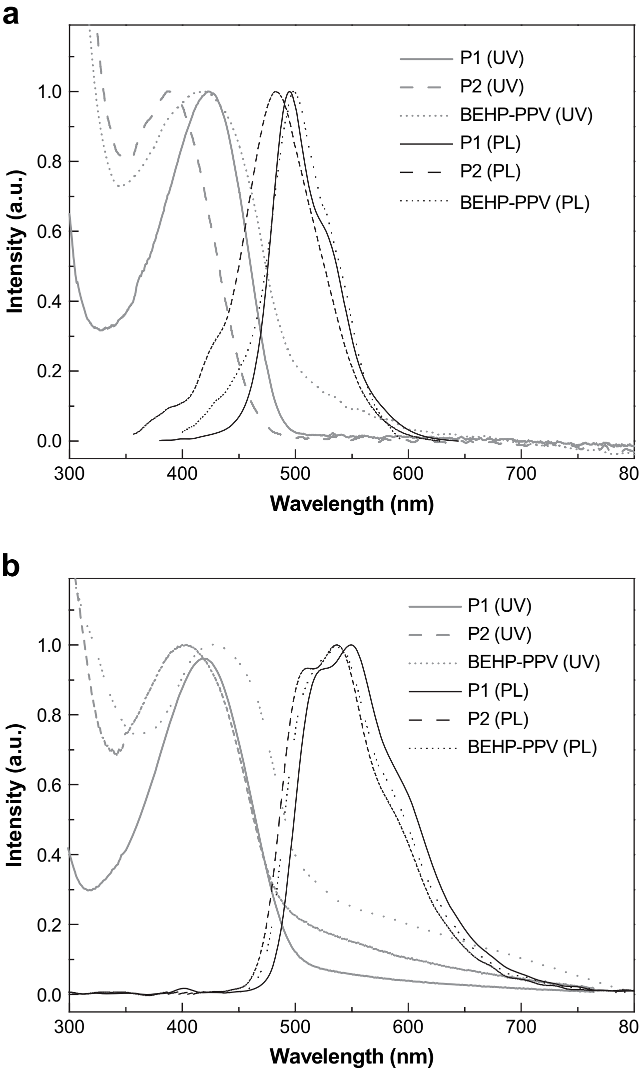

Fig. 2. UV–vis absorption and PL emission spectra of **P1** and **P2** in THF solution at a concentration of 1×10^{-5} mol/L (a) and solid thin film (b).

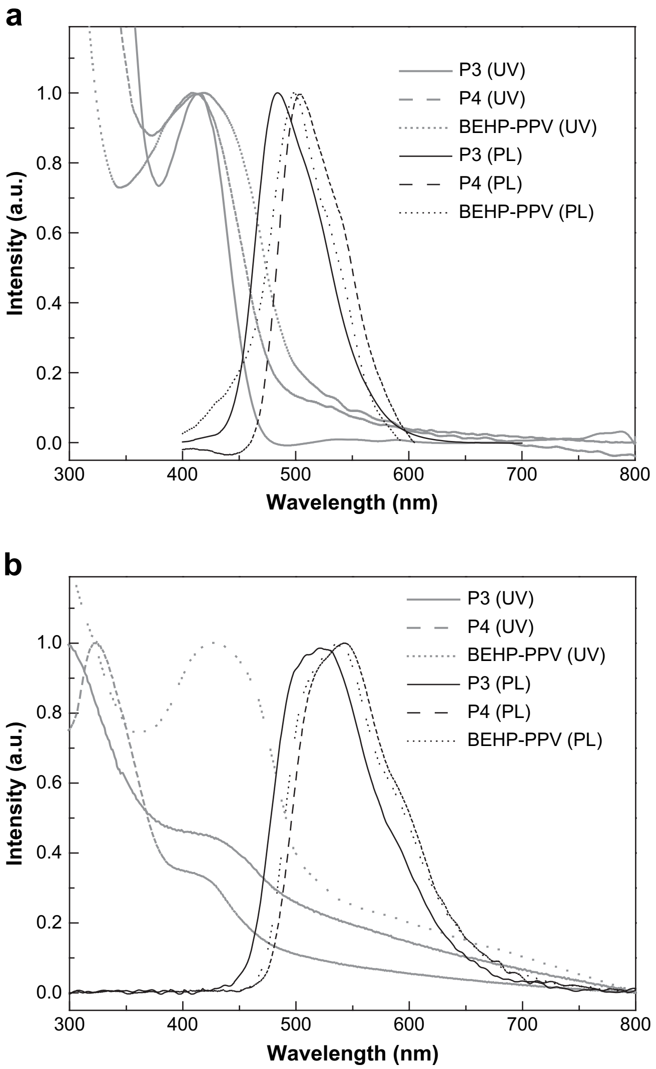

Fig. 3. UV–vis absorption and PL emission spectra of **P3** and **P4** in THF solution at a concentration of 1×10^{-5} mol/L (a) and solid thin film (b).

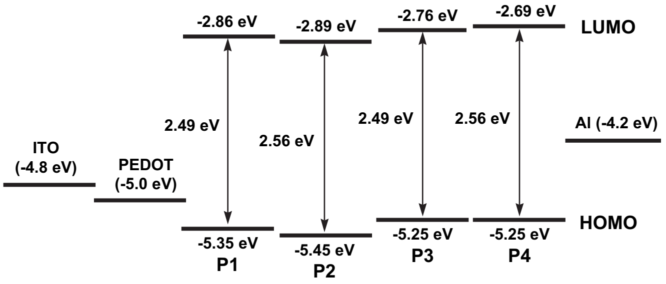

Fig. 4. Comparison of the energy levels of polymers with the work functions of the electrodes.

and 388 nm in THF solution, and at 419 and 404 nm as the solid thin film, respectively. The PL emission spectra of polymers showed a maximum peak at 495 and 482 nm in THF solution, and were red-shifted to 549 and 537 nm in the solid film state. The emission spectra in the solid film state were red-shifted over 50 nm, and the full width at half maximum (fwhm) was also 30 nm greater than solution conditions. The large red-shifted emission peaks of **P1** and **P2** in the solid film indicated that the inter-chain interaction, which can be attributed to the π–π^* transitions of conjugated polymer backbone, assisted the planarity of the polymer chain and increased the conjugation length in the solid state. As compared with **P1** and **P2** which have disilyl substituents, the introduction of a phenyl unit shows deriving shorter conjugation length of backbones, and in case of **P2** and BEHP–PPV, which have ter-phenyl units, it was not much different to the effects of conjugation length by alkoxy-phenyl and silyl-phenyl substituents.

Table 3
Electrochemical potentials and energy levels of polymers

Polymers	E_{onset}[a] (V)	HOMO[b] (eV)	LUMO[c] (eV)	E_g[d] (eV)
P1	0.55	−5.35	−2.86	2.49
P2	0.65	−5.45	−2.89	2.56
P3	0.45	−5.25	−2.76	2.49
P4	0.45	−5.25	−2.69	2.56

[a] Onset oxidation potential measured by cyclic voltammetry.
[b] Calculated from the oxidation potentials.
[c] Calculated from the HOMO energy levels and E_g.
[d] Energy band gap was estimated from the onset wavelength of the optical absorption.

The optical spectra of **P3** and **P4** are shown in Fig. 3. The maximum absorption peaks of **P3** and **P4** appeared at 413 and 409 nm in THF solution, and are red-shifted to around 425 and 418 nm as the solid thin film. The solid film spectra, compared to solution state, were also red-shifted due to intermolecular interactions between the conjugated polymer backbones. The PL emission spectra of **P3** and **P4** show maximum peaks at 485 and 503 nm in THF solution and at 521 and 543 nm in the solid film state. The emission spectra in the solid film state are red-shifted over 40 nm, with the fwhm 30 nm over the solution conditions. As compared with **P3** and **P4** which have penta-phenyl substituents, the fluorenyl units introduced conjugation lengths of backbones shorter than bis-phenyl units, and in case of BEHP–PPV and **P4**, which have alkoxy ter-phenyl and penta-phenyl units, it was not much different from the effects of conjugation length by alkoxy ter-phenyl and penta-phenyl substituents.

3.3. Electrochemical properties of the polymers

The electrochemical properties of the polymers were determined from the band gaps estimated from the absorption edges and the HOMO energy levels, which were estimated from cyclic voltammetry (CV). The CV was performed with a solution of

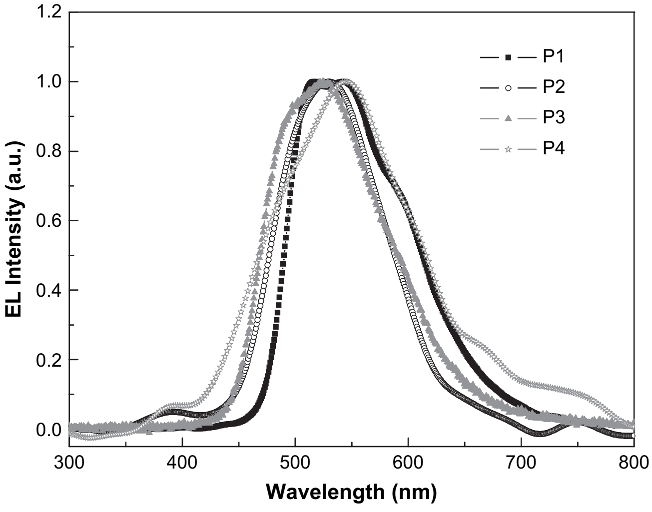

Fig. 5. Electroluminescence spectra of devices with the configuration of ITO/PEDOT/polymer/Al.

tetrabutylammonium tetrafluoroborate (Bu_4NBF_4) (0.10 M) in acetonitrile at a scan rate of 100 mV/s at room temperature under the protection of argon. A platinum electrode (~0.05 cm^2) coated with a thin polymer film was used as the working electrode. Pt wire and an $Ag/AgNO_3$ electrode were used as the counter and reference electrodes, respectively. The energy level of the $Ag/AgNO_3$ reference electrode (calibrated by the FC/FC^+ redox system) was 4.8 eV below the vacuum level. HOMO levels were calculated according to the empirical formula ($E_{HOMO} = -([E_{onset}]^{ox} + 4.8)$ (eV)). The oxidation potentials derived from the onset of electrochemical p-doping are summarized in Table 3. During the anodic scan, the oxidation onset potentials of **P1**–**P4** were in the range of 0.45–0.65 V, and exhibited irreversible p-doping process. HOMO energy levels of the present polymers were between −5.25 eV and −5.45 eV. The absorption onset wavelength of **P1**–**P4** was observed to be 485–498 nm in the solid thin film, corresponding to the band gap of 2.49–2.56 eV. The LUMO energy level was calculated from the values of the band gap and HOMO energy level, and the values were −2.69 eV to −2.89 eV (Fig. 4).

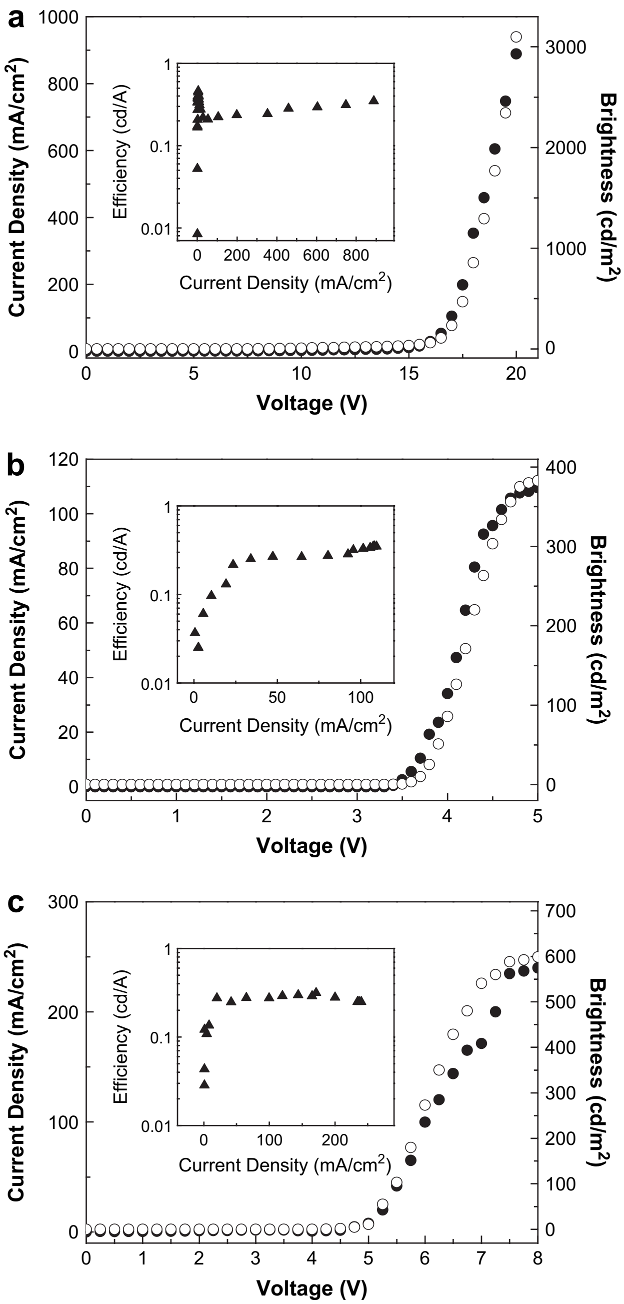

Fig. 6. Current density–voltage–luminescence (*J*–*V*–*L*) characteristics and efficiency of PLEDs of **P1** (a), **P2** (b) and **P3** (c) with the configuration of ITO/PEDOT/polymer/Al (●: current density; ○: brightness; ▲: efficiency).

Table 4
Device performance characteristics of polymers

Polymers	EL λ_{max} (nm)	Turn-on voltage (V)	Voltage[a] (V)	Current density[a] (mA/cm^2)	Luminance[b] (cd/m^2)	LE_{max}[a] (cd/A)	CIE[c] (*x*,*y*)
1	517, 542	16	20	888	3098	0.35	(0.37, 0.55)
2	530	3.6	5	110	383	0.35	(0.30, 0.51)
3	529	4.5	7	171	599	0.32	(0.30, 0.49)

[a] Measured under the condition of maximum luminescence efficiency.
[b] Maximum brightness.
[c] Calculated from the EL spectrum.

3.4. *EL property and current density–voltage–luminescence* (J–V–L) *characteristics*

The electroluminescence (EL) performance of the polymers was examined in the device configuration of ITO/PEDOT:PSS/polymer/Al. The typical EL spectra from such device are shown in Fig. 5. The EL spectra of the polymers were nearly the same as the PL of the polymers indicating that the EL and PL phenomena originated from the same excited state. The EL spectrum of **P1** shows two maximum peaks at 517 and 542 nm. In the case of **P2** and **P3**, the maximum peaks exhibited at 530 nm, and the maximum peak of **P4** was shown at 546 nm. As compared to the PL spectrum of the thin film, the EL spectrum of the polymer showed a decreased sub-peak and increased fwhm. For these polymers, aggregation potentially occurs mainly within the polymer chain *via* an intermolecular interaction between phenyl substituents. The effective conjugation length and color of the polymer can be controlled by utilizing several types of substituents. Substituents can increase the effective conjugation length by enforcing more coplanarity (or by restricting mobility) or decrease by disturbing coplanarity of the conjugated repeat units, act as electron donors or acceptors due purely to this electronic influence, and display some steric and some electronic effects simultaneously, which can both act in the same directions or in the opposite ones. Although alkoxy groups in PPV derivatives can increase the effective conjugation length caused by the electron-donating effect, being substituted with phenyl group, the electron-donating effect did not exercise an influence on the conjugated backbone. Moreover, the phenyl substituents induced aggregation due to the increase of intermolecular interaction.

The current density–voltage–luminescence (*J*–*V*–*L*) characteristics and electroluminescence efficiency of the devices fabricated from **P1**–**P3** are shown in Fig. 6 and Table 4. In case of **P4**, the properties of the device were not detected by low device performance due to low solubility. In the forward bias, the turn-on voltages of ITO/PEDOT/polymer/Al devices were 3.6–16 V. Since there is not much difference of HOMO/LUMO levels out of the three polymers, it is quite hard to deduce any direct relationship between the energy levels and the device characteristics including turn-on voltages and luminances. The luminescence intensities of the polymers increased with an increase in voltage and the maximum luminescence (L_{max}) of **P1** was 3098 cd/m^2 at 20 V. The luminescence efficiencies of the polymers at room temperature were between 0.32 and 0.35 cd/A. Therefore, the various phenyl substituents, which induce intermolecular interaction in the solid state, can introduce color tuning and device performance enhancement of the conjugated polymer as the emissive layer in PLED.

4. Conclusion

We present here the synthesis of novel conjugated polymers, **P1**–**P3**, which exhibit interesting properties for the development of PLED. **P1**–**P3** had characteristic absorption and emission peaks due to steric hindrance and intermolecular interaction of the phenyl substituents. The more phenyl substituents in the disilyl groups show deriving shorter conjugation lengths of backbones, and in the case of penta-phenyl PPV, the fluorenyl units introduced shorter conjugation lengths of backbones than bis-phenyl units. Moreover, there was little difference in the effects of conjugation length between alkoxy-phenyl and silyl-phenyl substituents, or alkoxy-ter-phenyl and penta-phenyl substituents. The HOMO energy levels of the polymers were −5.25 eV to −5.45 eV, and the LUMO energy levels at −2.69 eV to −2.89 eV. The polymer LEDs with the configuration of ITO/PEDOT/polymer/Al emitted light with maximum peaks at 517–546 nm. The maximum luminescence ($L_{\max}$) of **P1** was 3098 cd/m^2 at 20 V. The luminescence efficiencies of the polymers at room temperature were between 0.32 and 0.35 cd/A. The phenyl substituents with intermolecular interaction may result in an amorphous solid state, which gives decent device performance. The various phenyl substituents, which induce intermolecular interaction in the solid state, can introduce the color tuning and device performance improving of the conjugated polymer as the emissive layer in PLED.

Acknowledgements

This work was supported by the Ministry of Information and Communication, Korea, under the Information Technology Research Center (ITRC) Support Program.

References

[1] Tang CW, VanSlyke SA. Appl Phys Lett 1987;51:913–5.
[2] Bernius MT, Inbasekaran M, O'Brien J, Wu W. Adv Mater 2000;12:1737–50.
[3] Hancock JM, Gifford AP, Zhu Y, Lou Y, Jenekhe SA. Chem Mater 2006;18:4924–32.
[4] Sheats JR, Antoniadis H, Hueschen M, Leonard W, Miller J, Moon R, et al. Science 1996;273:884–8.
[5] Friend RH, Gymer RW, Holmes AB, Burroughes JH, Marks RN, Taliani C, et al. Nature 1999;397:121–8.
[6] Mikroyannidis JA, Gibbons KM, Kulkarni AP, Jenekhe SA. Macromolecules 2008;41:663–74.
[7] Yang R, Tian R, Hou Q, Yang W, Cao Y. Macromolecules 2003;36:7453–60.
[8] Lahti PM, Sarker A, Garay RO, Lenz RW, Karasz FE. Polymer 1994;35:1312–6.
[9] Chen ZK, Lee NHS, Huang W, Xu Y-S, Cao Y. Macromolecules 2003;36:1009–20.
[10] Burroughes JH, Bradley DDC, Brown AR, Marks RN, Mackay K, Friend RH, et al. Nature 1990;347:539–41.
[11] Gustafsson G, Cao Y, Treacy GM, Klavetter F, Colaneri N, Heeeger AJ. Nature 1992;357:477–9.
[12] Salbeck J, Bunsenges B. Phys Chem 1996;100:1666–77.
[13] Hwang D-H, Kim ST, Shim HK, Holmes AB, Moratti SC, Friend RH. Chem Commun 1996:2241–2.
[14] Johansson DM, Srdanov G, Yu G, Theander M, Inganäs O, Andersson MR. Macromolecules 2000;33:2525–9.
[15] Lee SH, Jang BB, Tsutsui T. Macromolecules 2002;35:1356–64.
[16] Gurge RM, Sarker A, Lahti PM, Hu B, Karasz FE. Macromolecules 1996;29:4287–92.
[17] Gurge RM, Sarker AM, Lahti PM, Hu B, Karasz FE. Macromolecules 1997;30:8286–92.
[18] Jin Y, Kim J, Lee S, Kim JY, Park SH, Lee K, et al. Macromolecules 2004;37:6711–5.
[19] Jin Y, Jee J, Kim K, Kim J, Song S, Park SH, et al. Polymer 2007;48:1541–9.
[20] Jin Y, Ju J, Kim J, Lee S, Kim JY, Park SH, et al. Macromolecules 2003;36:6970–5.
[21] Greenham NC, Moratti SC, Bradley DDC, Friend RH, Holmes AB. Nature 1993;365:628–30.
[22] Gustafsson G, Treacy GM, Cao Y, Klavetter F, Colaneri N, Heeger AJ. Synth Met 1993;55–57:4123–7.
[23] Zhang C, Höger S, Pakbaz K, Wudl F, Heeger AJ. J Electron Mater 1993;22:413–7.
[24] Zhang C, Braun D, Heeger AJ. J Appl Phys 1993;73:5177–80.
[25] Jin Y, Kim JY, Song S, Xia Y, Kim J, Woo HY, et al. Polymer 2008;49:467–73.
[26] Grem G, Leditzky G, Ullrich B, Leising G. Synth Met 1992;51:383–9.
[27] Braun D, Starting EGJ, Demandt RCJE, Rikken GLJ, Kessener YARR, Venhuizen AHJ. Synth Met 1994;66:75–9.
[28] Tang R, Tan Z, Cheng C, Li Y, Xi F. Polymer 2005;46:5341–50.
[29] Jin Y, Kim JY, Park SH, Kim J, Lee S, Lee K, et al. Polymer 2005;46:12158–65.
[30] Zhen H, Xu W, Yang W, Chen Q, Xu Y, Jiang J, et al. Macromol Rapid Commun 2006;27:2095–100.
[31] Ferreira M, Constantino CJL, Olivati CA, Balogh DT, Aroca RF, Faria RM, et al. Polymer 2005;46:5140–8.
[32] Halls JJM, Arias AC, MacKenzie JD, Wu W, Inbasekaran M, Woo ED, et al. Adv Mater 2000;12:498–502.
[33] Campoy-Quiles M, Etchegoin PG, Bradley DDC. Phys Rev B 2005;72:45209.
[34] Wood P, Samuel IDW, Webster GR, Burn PL. Synth Met 2001;119:571–2.
[35] Shirota Y. J Mater Chem 2005;15:75–93.
[36] Konstandakopoulou FD, Iconomopoulou SM, Gravalos KG, Kallitsis JK. Chem Mater 2000;12:2957–63.
[37] Becker H, Burns SE, Friend RH. Phys Rev B 1997;56:1893–905.
[38] Scott JC, Karg S, Carter SA. J Appl Phys 1997;82:1454–60.
[39] Jin Y, Kim J, Park SH, Kim H, Lee K, Suh H. Bull Korean Chem Soc 2005;26:1807–18.